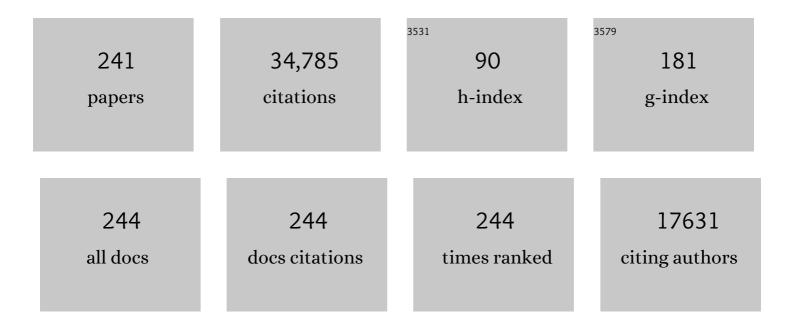
## Wenxing Chen

List of Publications by Year in descending order

Source: https://exaly.com/author-pdf/2236115/publications.pdf Version: 2024-02-01



| #  | Article  | IF   | CITATIONS |
|----|--|------|-----------|
| 1  | Isolated Single Iron Atoms Anchored on Nâ€Doped Porous Carbon as an Efficient Electrocatalyst for<br>the Oxygen Reduction Reaction. Angewandte Chemie - International Edition, 2017, 56, 6937-6941.  | 13.8 | 1,542     |
| 2  | General synthesis and definitive structural identification of MN4C4 single-atom catalysts with tunable electrocatalytic activities. Nature Catalysis, 2018, 1, 63-72.  | 34.4 | 1,476     |
| 3  | Design of N-Coordinated Dual-Metal Sites: A Stable and Active Pt-Free Catalyst for Acidic Oxygen<br>Reduction Reaction. Journal of the American Chemical Society, 2017, 139, 17281-17284.  | 13.7 | 1,220     |
| 4  | lonic Exchange of Metal–Organic Frameworks to Access Single Nickel Sites for Efficient<br>Electroreduction of CO <sub>2</sub> . Journal of the American Chemical Society, 2017, 139, 8078-8081.  | 13.7 | 1,115     |
| 5  | Design of Single-Atom Co–N <sub>5</sub> Catalytic Site: A Robust Electrocatalyst for CO <sub>2</sub><br>Reduction with Nearly 100% CO Selectivity and Remarkable Stability. Journal of the American Chemical<br>Society, 2018, 140, 4218-4221. | 13.7 | 945       |
| 6  | Regulation of Coordination Number over Single Co Sites: Triggering the Efficient Electroreduction of CO <sub>2</sub> . Angewandte Chemie - International Edition, 2018, 57, 1944-1948.   | 13.8 | 888       |
| 7  | Engineering the electronic structure of single atom Ru sites via compressive strain boosts acidic water oxidation electrocatalysis. Nature Catalysis, 2019, 2, 304-313.  | 34.4 | 757       |
| 8  | Defect Effects on TiO <sub>2</sub> Nanosheets: Stabilizing Single Atomic Site Au and Promoting<br>Catalytic Properties. Advanced Materials, 2018, 30, 1705369.   | 21.0 | 751       |
| 9  | Direct transformation of bulk copper into copper single sites via emitting and trapping of atoms.<br>Nature Catalysis, 2018, 1, 781-786.   | 34.4 | 746       |
| 10 | Direct observation of noble metal nanoparticles transforming to thermally stable single atoms.<br>Nature Nanotechnology, 2018, 13, 856-861.  | 31.5 | 741       |
| 11 | Enhanced oxygen reduction with single-atomic-site iron catalysts for a zinc-air battery and hydrogen-air fuel cell. Nature Communications, 2018, 9, 5422.  | 12.8 | 696       |
| 12 | Uncoordinated Amine Groups of Metal–Organic Frameworks to Anchor Single Ru Sites as<br>Chemoselective Catalysts toward the Hydrogenation of Quinoline. Journal of the American Chemical<br>Society, 2017, 139, 9419-9422.                      | 13.7 | 558       |
| 13 | Hollow N-Doped Carbon Spheres with Isolated Cobalt Single Atomic Sites: Superior Electrocatalysts for Oxygen Reduction. Journal of the American Chemical Society, 2017, 139, 17269-17272.  | 13.7 | 556       |
| 14 | Engineering unsymmetrically coordinated Cu-S1N3 single atom sites with enhanced oxygen reduction activity. Nature Communications, 2020, 11, 3049.  | 12.8 | 537       |
| 15 | Matching the kinetics of natural enzymes with a single-atom iron nanozyme. Nature Catalysis, 2021, 4, 407-417.   | 34.4 | 517       |
| 16 | Fe Isolated Single Atoms on S, N Codoped Carbon by Copolymer Pyrolysis Strategy for Highly Efficient<br>Oxygen Reduction Reaction. Advanced Materials, 2018, 30, e1800588.   | 21.0 | 511       |
| 17 | Bismuth Single Atoms Resulting from Transformation of Metal–Organic Frameworks and Their Use as<br>Electrocatalysts for CO <sub>2</sub> Reduction. Journal of the American Chemical Society, 2019, 141,<br>16569-16573.                        | 13.7 | 501       |
| 18 | Single-atom tailoring of platinum nanocatalysts for high-performance multifunctional electrocatalysis. Nature Catalysis, 2019, 2, 495-503.   | 34.4 | 464       |

| #  | Article   | IF   | CITATIONS |
|----|---|------|-----------|
| 19 | lridium single-atom catalyst on nitrogen-doped carbon for formic acid oxidation synthesized using a<br>general host–guest strategy. Nature Chemistry, 2020, 12, 764-772.  | 13.6 | 452       |
| 20 | Atomicâ€Level Modulation of Electronic Density at Cobalt Singleâ€Atom Sites Derived from<br>Metal–Organic Frameworks: Enhanced Oxygen Reduction Performance. Angewandte Chemie -<br>International Edition, 2021, 60, 3212-3221.                 | 13.8 | 445       |
| 21 | Rational Design of Single Molybdenum Atoms Anchored on Nâ€Doped Carbon for Effective Hydrogen<br>Evolution Reaction. Angewandte Chemie - International Edition, 2017, 56, 16086-16090.  | 13.8 | 431       |
| 22 | Tuning defects in oxides at roomÂtemperature by lithium reduction. Nature Communications, 2018, 9,<br>1302.   | 12.8 | 428       |
| 23 | Single Tungsten Atoms Supported on MOFâ€Derived Nâ€Doped Carbon for Robust Electrochemical<br>Hydrogen Evolution. Advanced Materials, 2018, 30, e1800396.   | 21.0 | 427       |
| 24 | Single-atom Rh/N-doped carbon electrocatalyst for formic acid oxidation. Nature Nanotechnology, 2020, 15, 390-397.  | 31.5 | 420       |
| 25 | Isolated Single-Atom Pd Sites in Intermetallic Nanostructures: High Catalytic Selectivity for Semihydrogenation of Alkynes. Journal of the American Chemical Society, 2017, 139, 7294-7301.   | 13.7 | 354       |
| 26 | Engineering the Atomic Interface with Single Platinum Atoms for Enhanced Photocatalytic Hydrogen<br>Production. Angewandte Chemie - International Edition, 2020, 59, 1295-1301.   | 13.8 | 344       |
| 27 | Electronic structure engineering to boost oxygen reduction activity by controlling the coordination of the central metal. Energy and Environmental Science, 2018, 11, 2348-2352.  | 30.8 | 336       |
| 28 | Single-atomic cobalt sites embedded in hierarchically ordered porous nitrogen-doped carbon as a superior bifunctional electrocatalyst. Proceedings of the National Academy of Sciences of the United States of America, 2018, 115, 12692-12697. | 7.1  | 325       |
| 29 | A general synthesis approach for amorphous noble metal nanosheets. Nature Communications, 2019,<br>10, 4855.  | 12.8 | 321       |
| 30 | Inâ€Situ Thermal Atomization To Convert Supported Nickel Nanoparticles into Surfaceâ€Bound Nickel<br>Singleâ€Atom Catalysts. Angewandte Chemie - International Edition, 2018, 57, 14095-14100.  | 13.8 | 310       |
| 31 | Isolated Single Iron Atoms Anchored on Nâ€Doped Porous Carbon as an Efficient Electrocatalyst for the Oxygen Reduction Reaction. Angewandte Chemie, 2017, 129, 7041-7045.   | 2.0  | 306       |
| 32 | Boosting Oxygen Reduction Catalysis with Fe–N <sub>4</sub> Sites Decorated Porous Carbons<br>toward Fuel Cells. ACS Catalysis, 2019, 9, 2158-2163.  | 11.2 | 297       |
| 33 | A general route <i>via</i> formamide condensation to prepare atomically dispersed<br>metal–nitrogen–carbon electrocatalysts for energy technologies. Energy and Environmental Science,<br>2019, 12, 1317-1325.                                  | 30.8 | 290       |
| 34 | High-Concentration Single Atomic Pt Sites on Hollow CuSx for Selective O2 Reduction to H2O2 in Acid Solution. CheM, 2019, 5, 2099-2110.   | 11.7 | 279       |
| 35 | Carbon nitride supported Fe2 cluster catalysts with superior performance for alkene epoxidation.<br>Nature Communications, 2018, 9, 2353.   | 12.8 | 278       |
| 36 | Atomic interface effect of a single atom copper catalyst for enhanced oxygen reduction reactions.<br>Energy and Environmental Science, 2019, 12, 3508-3514.   | 30.8 | 278       |

| #  | Article   | IF   | CITATIONS |
|----|---|------|-----------|
| 37 | Solid-Diffusion Synthesis of Single-Atom Catalysts Directly from Bulk Metal for Efficient CO2<br>Reduction. Joule, 2019, 3, 584-594.  | 24.0 | 277       |
| 38 | Directly transforming copper (I) oxide bulk into isolated single-atom copper sites catalyst through gas-transport approach. Nature Communications, 2019, 10, 3734.  | 12.8 | 276       |
| 39 | A Polymer Encapsulation Strategy to Synthesize Porous Nitrogenâ€Doped Carbonâ€Nanosphereâ€Supported<br>Metal Isolatedâ€Singleâ€Atomicâ€Site Catalysts. Advanced Materials, 2018, 30, e1706508.  | 21.0 | 266       |
| 40 | Accelerating water dissociation kinetics by isolating cobalt atoms into ruthenium lattice. Nature Communications, 2018, 9, 4958.  | 12.8 | 264       |
| 41 | In Situ Phosphatizing of Triphenylphosphine Encapsulated within Metal–Organic Frameworks to<br>Design Atomic Co <sub>1</sub> –P <sub>1</sub> N <sub>3</sub> Interfacial Structure for Promoting<br>Catalytic Performance. Journal of the American Chemical Society, 2020, 142, 8431-8439. | 13.7 | 259       |
| 42 | Confined Pyrolysis within Metal–Organic Frameworks To Form Uniform Ru <sub>3</sub> Clusters for<br>Efficient Oxidation of Alcohols. Journal of the American Chemical Society, 2017, 139, 9795-9798.   | 13.7 | 258       |
| 43 | Metal (Hydr)oxides@Polymer Core–Shell Strategy to Metal Single-Atom Materials. Journal of the<br>American Chemical Society, 2017, 139, 10976-10979.   | 13.7 | 257       |
| 44 | Cation vacancy stabilization of single-atomic-site Pt1/Ni(OH)x catalyst for diboration of alkynes and alkenes. Nature Communications, 2018, 9, 1002.  | 12.8 | 255       |
| 45 | Engineering Isolated Mn–N <sub>2</sub> C <sub>2</sub> Atomic Interface Sites for Efficient<br>Bifunctional Oxygen Reduction and Evolution Reaction. Nano Letters, 2020, 20, 5443-5450.  | 9.1  | 249       |
| 46 | Discovery of main group single Sb–N <sub>4</sub> active sites for CO <sub>2</sub> electroreduction to formate with high efficiency. Energy and Environmental Science, 2020, 13, 2856-2863.  | 30.8 | 245       |
| 47 | Regulation of Coordination Number over Single Co Sites: Triggering the Efficient Electroreduction of CO <sub>2</sub> . Angewandte Chemie, 2018, 130, 1962-1966.   | 2.0  | 244       |
| 48 | Design of a Singleâ€Atom Indium <sup>Î′+</sup> –N <sub>4</sub> Interface for Efficient Electroreduction<br>of CO <sub>2</sub> to Formate. Angewandte Chemie - International Edition, 2020, 59, 22465-22469.   | 13.8 | 232       |
| 49 | Atomically Dispersed Copper–Platinum Dual Sites Alloyed with Palladium Nanorings Catalyze the<br>Hydrogen Evolution Reaction. Angewandte Chemie - International Edition, 2017, 56, 16047-16051.   | 13.8 | 231       |
| 50 | Atomically dispersed Au1 catalyst towards efficient electrochemical synthesis of ammonia. Science<br>Bulletin, 2018, 63, 1246-1253.   | 9.0  | 225       |
| 51 | Design of ultrathin Pt-Mo-Ni nanowire catalysts for ethanol electrooxidation. Science Advances, 2017,<br>3, e1603068.   | 10.3 | 224       |
| 52 | Regulating the coordination environment of Co single atoms for achieving efficient electrocatalytic activity in CO2 reduction. Applied Catalysis B: Environmental, 2019, 240, 234-240.  | 20.2 | 224       |
| 53 | Discovering Partially Charged Single-Atom Pt for Enhanced Anti-Markovnikov Alkene Hydrosilylation.<br>Journal of the American Chemical Society, 2018, 140, 7407-7410.   | 13.7 | 218       |
| 54 | Controlling N-doping type in carbon to boost single-atom site Cu catalyzed transfer hydrogenation of quinoline. Nano Research, 2020, 13, 3082-3087.   | 10.4 | 215       |

| #  | Article  | IF   | CITATIONS |
|----|--|------|-----------|
| 55 | A cocoon silk chemistry strategy to ultrathin N-doped carbon nanosheet with metal single-site catalysts. Nature Communications, 2018, 9, 3861.   | 12.8 | 210       |
| 56 | A single-atom Fe–N <sub>4</sub> catalytic site mimicking bifunctional antioxidative enzymes for oxidative stress cytoprotection. Chemical Communications, 2019, 55, 159-162.   | 4.1  | 209       |
| 57 | Efficient and Robust Hydrogen Evolution: Phosphorus Nitride Imide Nanotubes as Supports for<br>Anchoring Single Ruthenium Sites. Angewandte Chemie - International Edition, 2018, 57, 9495-9500.   | 13.8 | 205       |
| 58 | Temperature-Controlled Selectivity of Hydrogenation and Hydrodeoxygenation in the Conversion of<br>Biomass Molecule by the Ru <sub>1</sub> /mpg-C <sub>3</sub> N <sub>4</sub> Catalyst. Journal of the<br>American Chemical Society, 2018, 140, 11161-11164. | 13.7 | 199       |
| 59 | Single-Atom Co–N <sub>4</sub> Electrocatalyst Enabling Four-Electron Oxygen Reduction with<br>Enhanced Hydrogen Peroxide Tolerance for Selective Sensing. Journal of the American Chemical<br>Society, 2020, 142, 16861-16867.                               | 13.7 | 184       |
| 60 | Gramâ€Scale Synthesis of Highâ€Loading Singleâ€Atomicâ€Site Fe Catalysts for Effective Epoxidation of<br>Styrene. Advanced Materials, 2020, 32, e2000896.  | 21.0 | 181       |
| 61 | Engineering of Coordination Environment and Multiscale Structure in Single-Site Copper Catalyst for<br>Superior Electrocatalytic Oxygen Reduction. Nano Letters, 2020, 20, 6206-6214.  | 9.1  | 178       |
| 62 | Cactus-like NiCo2S4@NiFe LDH hollow spheres as an effective oxygen bifunctional electrocatalyst in alkaline solution. Applied Catalysis B: Environmental, 2021, 286, 119869.   | 20.2 | 176       |
| 63 | Isolated Ni Atoms Dispersed on Ru Nanosheets: High-Performance Electrocatalysts toward Hydrogen<br>Oxidation Reaction. Nano Letters, 2020, 20, 3442-3448.  | 9.1  | 172       |
| 64 | Isolated Fe and Co dual active sites on nitrogen-doped carbon for a highly efficient oxygen reduction reaction. Chemical Communications, 2018, 54, 4274-4277.  | 4.1  | 166       |
| 65 | Ordered Porous Nitrogenâ€Doped Carbon Matrix with Atomically Dispersed Cobalt Sites as an Efficient<br>Catalyst for Dehydrogenation and Transfer Hydrogenation of Nâ€Heterocycles. Angewandte Chemie -<br>International Edition, 2018, 57, 11262-11266.      | 13.8 | 165       |
| 66 | Atomically Dispersed Ruthenium Species Inside Metal–Organic Frameworks: Combining the High<br>Activity of Atomic Sites and the Molecular Sieving Effect of MOFs. Angewandte Chemie - International<br>Edition, 2019, 58, 4271-4275.                          | 13.8 | 162       |
| 67 | Hierarchical Fe-doped NiO x nanotubes assembled from ultrathin nanosheets containing trivalent nickel for oxygen evolution reaction. Nano Energy, 2017, 38, 167-174.   | 16.0 | 160       |
| 68 | Dual-atom Pt heterogeneous catalyst with excellent catalytic performances for the selective hydrogenation and epoxidation. Nature Communications, 2021, 12, 3181.  | 12.8 | 156       |
| 69 | Single-atom Ni-N4 provides a robust cellular NO sensor. Nature Communications, 2020, 11, 3188.   | 12.8 | 153       |
| 70 | Mesoporous Nitrogenâ€Doped Carbonâ€Nanosphereâ€Supported Isolated Singleâ€Atom Pd Catalyst for Highly<br>Efficient Semihydrogenation of Acetylene. Advanced Materials, 2019, 31, e1901024.   | 21.0 | 146       |
| 71 | MOFâ€Confined Subâ€2 nm Atomically Ordered Intermetallic PdZn Nanoparticles as Highâ€Performance<br>Catalysts for Selective Hydrogenation of Acetylene. Advanced Materials, 2018, 30, e1801878.  | 21.0 | 133       |
| 72 | Atomically Dispersed Ru on Ultrathin Pd Nanoribbons. Journal of the American Chemical Society, 2016,<br>138, 13850-13853.  | 13.7 | 132       |

| #  | Article   | IF   | CITATIONS |
|----|---|------|-----------|
| 73 | Simultaneous oxidative and reductive reactions in one system by atomic design. Nature Catalysis, 2021, 4, 134-143.  | 34.4 | 132       |
| 74 | Identification of Fenton-like active Cu sites by heteroatom modulation of electronic density.<br>Proceedings of the National Academy of Sciences of the United States of America, 2022, 119, .                          | 7.1  | 132       |
| 75 | N-Bridged Co–N–Ni: new bimetallic sites for promoting electrochemical CO <sub>2</sub> reduction.<br>Energy and Environmental Science, 2021, 14, 3019-3028.  | 30.8 | 128       |
| 76 | One-Pot Pyrolysis to N-Doped Graphene with High-Density Pt Single Atomic Sites as Heterogeneous<br>Catalyst for Alkene Hydrosilylation. ACS Catalysis, 2018, 8, 10004-10011.  | 11.2 | 121       |
| 77 | Isolating contiguous Pt atoms and forming Pt-Zn intermetallic nanoparticles to regulate selectivity in 4-nitrophenylacetylene hydrogenation. Nature Communications, 2019, 10, 3787.                                     | 12.8 | 119       |
| 78 | Porphyrin-like Fe-N4 sites with sulfur adjustment on hierarchical porous carbon for different rate-determining steps in oxygen reduction reaction. Nano Research, 2018, 11, 6260-6269.                                  | 10.4 | 118       |
| 79 | Engineering a metal–organic framework derived Mn–N <sub>4</sub> –C <sub>x</sub> S <sub>y</sub><br>atomic interface for highly efficient oxygen reduction reaction. Chemical Science, 2020, 11, 5994-5999.               | 7.4  | 113       |
| 80 | Complementary Operando Spectroscopy identification of in-situ generated metastable<br>charge-asymmetry Cu2-CuN3 clusters for CO2 reduction to ethanol. Nature Communications, 2022, 13,<br>1322.                        | 12.8 | 113       |
| 81 | Singleâ€Site Au <sup>I</sup> Catalyst for Silane Oxidation with Water. Advanced Materials, 2018, 30, 1704720.   | 21.0 | 112       |
| 82 | Scaleâ€Up Biomass Pathway to Cobalt Single‣ite Catalysts Anchored on Nâ€Doped Porous Carbon<br>Nanobelt with Ultrahigh Surface Area. Advanced Functional Materials, 2018, 28, 1802167.                                  | 14.9 | 112       |
| 83 | Hydrodeoxygenation of water-insoluble bio-oil to alkanes using a highly dispersed Pd–Mo catalyst.<br>Nature Communications, 2017, 8, 591.   | 12.8 | 110       |
| 84 | Atomically dispersed Fe atoms anchored on COF-derived N-doped carbon nanospheres as efficient multi-functional catalysts. Chemical Science, 2020, 11, 786-790.  | 7.4  | 110       |
| 85 | Two-Step Carbothermal Welding To Access Atomically Dispersed Pd <sub>1</sub> on Three-Dimensional<br>Zirconia Nanonet for Direct Indole Synthesis. Journal of the American Chemical Society, 2019, 141,<br>10590-10594. | 13.7 | 108       |
| 86 | Catalytic degradation of recalcitrant pollutants by Fenton-like process using<br>polyacrylonitrile-supported iron (II) phthalocyanine nanofibers: Intermediates and pathway. Water<br>Research, 2016, 93, 296-305.      | 11.3 | 106       |
| 87 | Negative Pressure Pyrolysis Induced Highly Accessible Single Sites Dispersed on 3D Graphene<br>Frameworks for Enhanced Oxygen Reduction. Angewandte Chemie - International Edition, 2020, 59,<br>20465-20469.           | 13.8 | 104       |
| 88 | Single-atom Fe with Fe1N3 structure showing superior performances for both hydrogenation and transfer hydrogenation of nitrobenzene. Science China Materials, 2021, 64, 642-650.  | 6.3  | 98        |
| 89 | Solvothermal Synthesis of Ternary Cu <sub>2</sub> MoS <sub>4</sub> Nanosheets: Structural Characterization at the Atomic Level. Small, 2014, 10, 4637-4644.   | 10.0 | 97        |
| 90 | Integrating single-cobalt-site and electric field of boron nitride in dechlorination electrocatalysts by bioinspired design. Nature Communications, 2021, 12, 303.  | 12.8 | 97        |

| #   | Article  | IF   | CITATIONS |
|-----|--|------|-----------|
| 91  | Rational Control of the Selectivity of a Ruthenium Catalyst for Hydrogenation of 4â€Nitrostyrene by<br>Strain Regulation. Angewandte Chemie - International Edition, 2017, 56, 11971-11975.  | 13.8 | 93        |
| 92  | Revealing the Active Species for Aerobic Alcohol Oxidation by Using Uniform Supported Palladium Catalysts. Angewandte Chemie - International Edition, 2018, 57, 4642-4646.   | 13.8 | 93        |
| 93  | Regulating the Catalytic Performance of Single-Atomic-Site Ir Catalyst for Biomass Conversion by<br>Metal–Support Interactions. ACS Catalysis, 2019, 9, 5223-5230.   | 11.2 | 87        |
| 94  | Tuning Polarity of Cu-O Bond in Heterogeneous Cu Catalyst to Promote Additive-free Hydroboration of Alkynes. CheM, 2020, 6, 725-737.   | 11.7 | 87        |
| 95  | Efficient Plasmonic Au/CdSe Nanodumbbell for Photoelectrochemical Hydrogen Generation beyond<br>Visible Region. Advanced Energy Materials, 2019, 9, 1803889.   | 19.5 | 85        |
| 96  | MnN <sub>4</sub> Oxygen Reduction Electrocatalyst: Operando Investigation of Active Sites and<br>High Performance in Zinc–Air Battery. Advanced Energy Materials, 2021, 11, 2002753.  | 19.5 | 83        |
| 97  | Rational Design of Single Molybdenum Atoms Anchored on Nâ€Doped Carbon for Effective Hydrogen<br>Evolution Reaction. Angewandte Chemie, 2017, 129, 16302-16306.  | 2.0  | 82        |
| 98  | Cation/Anion Exchange Reactions toward the Syntheses of Upgraded Nanostructures: Principles and Applications. Matter, 2020, 2, 554-586.  | 10.0 | 81        |
| 99  | In Situ Implanting of Single Tungsten Sites into Defective UiOâ€66(Zr) by Solventâ€Free Route for Efficient<br>Oxidative Desulfurization at Room Temperature. Angewandte Chemie - International Edition, 2021, 60,<br>20318-20324. | 13.8 | 81        |
| 100 | Single-Atom Au <sup>I</sup> –N <sub>3</sub> Site for Acetylene Hydrochlorination Reaction. ACS<br>Catalysis, 2020, 10, 1865-1870.  | 11.2 | 76        |
| 101 | Coordination structure dominated performance of single-atomic Pt catalyst for anti-Markovnikov<br>hydroboration of alkenes. Science China Materials, 2020, 63, 972-981.  | 6.3  | 74        |
| 102 | Room-Temperature Synthesis of Single Iron Site by Electrofiltration for Photoreduction of CO <sub>2</sub> into Tunable Syngas. ACS Nano, 2020, 14, 6164-6172.  | 14.6 | 71        |
| 103 | The consortium of heterogeneous cobalt phthalocyanine catalyst and bicarbonate ion as a novel platform for contaminants elimination based on peroxymonosulfate activation. Journal of Hazardous Materials, 2016, 301, 214-221.     | 12.4 | 66        |
| 104 | Fabricating Pd isolated single atom sites on C3N4/rGO for heterogenization of homogeneous catalysis. Nano Research, 2020, 13, 947-951.   | 10.4 | 65        |
| 105 | Self-floating graphitic carbon nitride/zinc phthalocyanine nanofibers for photocatalytic degradation of contaminants. Journal of Hazardous Materials, 2016, 317, 17-26.  | 12.4 | 64        |
| 106 | Silkâ€Derived 2D Porous Carbon Nanosheets with Atomicallyâ€Dispersed Feâ€N <i><sub>x</sub></i> Sites<br>for Highly Efficient Oxygen Reaction Catalysts. Small, 2019, 15, e1804966.   | 10.0 | 64        |
| 107 | Interfacial engineering of 3D hollow CoSe2@ultrathin MoSe2 core@shell heterostructure for efficient pH-universal hydrogen evolution reaction. Nano Research, 2022, 15, 2895-2904.  | 10.4 | 64        |
| 108 | In-situ polymerization induced atomically dispersed manganese sites as cocatalyst for CO2 photoreduction into synthesis gas. Nano Energy, 2020, 76, 105059.  | 16.0 | 60        |

| #   | Article  | IF   | CITATIONS |
|-----|--|------|-----------|
| 109 | Engineering the Atomic Interface with Single Platinum Atoms for Enhanced Photocatalytic Hydrogen<br>Production. Angewandte Chemie, 2020, 132, 1311-1317.   | 2.0  | 59        |
| 110 | Factors Influencing the Performance of Copper-Bearing Catalysts in the CO <sub>2</sub> Reduction System. ACS Energy Letters, 2021, 6, 3992-4022.   | 17.4 | 58        |
| 111 | Construction of MnO <sub>2</sub> Artificial Leaf with Atomic Thickness as Highly Stable Battery<br>Anodes. Advanced Materials, 2020, 32, e1906582.   | 21.0 | 57        |
| 112 | Graphitic Carbon Nitride from Burial to Re-emergence on Polyethylene Terephthalate Nanofibers as an<br>Easily Recycled Photocatalyst for Degrading Antibiotics under Solar Irradiation. ACS Applied<br>Materials & Interfaces, 2016, 8, 25962-25970. | 8.0  | 56        |
| 113 | Ultrafast Rechargeable Aqueous Zincâ€lon Batteries Based on Stable Radical Chemistry. Advanced<br>Functional Materials, 2021, 31, 2102011.   | 14.9 | 56        |
| 114 | Promoting electrocatalytic methanol oxidation of platinum nanoparticles by cerium modification.<br>Nano Energy, 2020, 73, 104784.  | 16.0 | 54        |
| 115 | Atomically Dispersed Copper–Platinum Dual Sites Alloyed with Palladium Nanorings Catalyze the<br>Hydrogen Evolution Reaction. Angewandte Chemie, 2017, 129, 16263-16267.   | 2.0  | 53        |
| 116 | Highly Selective Photoreduction of CO <sub>2</sub> with Suppressing H <sub>2</sub> Evolution by<br>Plasmonic Au/CdSe–Cu <sub>2</sub> O Hierarchical Nanostructures under Visible Light. Small, 2020,<br>16, e2000426.                                | 10.0 | 53        |
| 117 | Simultaneous diffusion of cation and anion to access N, S co-coordinated Bi-sites for enhanced CO2 electroreduction. Nano Research, 2021, 14, 2790-2796.   | 10.4 | 53        |
| 118 | Construction of Dualâ€Activeâ€5ite Copper Catalyst Containing both CuN <sub>3</sub> and<br>CuN <sub>4</sub> Sites. Small, 2021, 17, e2006834.  | 10.0 | 52        |
| 119 | Electrodeposition of polypyrrole on carbon nanotube-coated cotton fabrics for all-solid flexible supercapacitor electrodes. RSC Advances, 2016, 6, 13359-13364.  | 3.6  | 51        |
| 120 | Bimetallic Ru–Co Clusters Derived from a Confined Alloying Process within Zeolite–Imidazolate<br>Frameworks for Efficient NH <sub>3</sub> Decomposition and Synthesis. ACS Applied Materials &<br>Interfaces, 2017, 9, 39450-39455.                  | 8.0  | 51        |
| 121 | Single atom catalysts by atomic diffusion strategy. Nano Research, 2021, 14, 4398-4416.  | 10.4 | 51        |
| 122 | Single copper sites dispersed on hierarchically porous carbon for improving oxygen reduction reaction towards zinc-air battery. Nano Research, 2021, 14, 998-1003.   | 10.4 | 50        |
| 123 | Sub-nm ruthenium cluster as an efficient and robust catalyst for decomposition and synthesis of ammonia: Break the "size shackles― Nano Research, 2018, 11, 4774-4785.   | 10.4 | 49        |
| 124 | Carbon-supported high-entropy Co-Zn-Cd-Cu-Mn sulfide nanoarrays promise high-performance overall water splitting. Nano Research, 2022, 15, 6054-6061.  | 10.4 | 47        |
| 125 | Atomic regulation of metal–organic framework derived carbon-based single-atom catalysts for the electrochemical CO <sub>2</sub> reduction reaction. Journal of Materials Chemistry A, 2021, 9, 23382-23418.  | 10.3 | 46        |
| 126 | Single iron atoms coordinated to g-C <sub>3</sub> N <sub>4</sub> on hierarchical porous N-doped carbon polyhedra as a high-performance electrocatalyst for the oxygen reduction reaction. Chemical Communications, 2020, 56, 798-801.                | 4.1  | 45        |

| #   | Article  | IF   | CITATIONS |
|-----|--|------|-----------|
| 127 | Engineering Ag–N <i><sub>x</sub></i> Single-Atom Sites on Porous Concave N-Doped Carbon for<br>Boosting CO <sub>2</sub> Electroreduction. ACS Applied Materials & Interfaces, 2021, 13,<br>17736-17744.        | 8.0  | 45        |
| 128 | Key role of activated carbon fibers in enhanced decomposition of pollutants using heterogeneous<br>cobalt/peroxymonosulfate system. Journal of Chemical Technology and Biotechnology, 2016, 91,<br>1257-1265.  | 3.2  | 44        |
| 129 | Mesoporous S doped Fe–N–C materials as highly active oxygen reduction reaction catalyst. Chemical<br>Communications, 2018, 54, 12073-12076.  | 4.1  | 44        |
| 130 | Atomicâ€Level Modulation of Electronic Density at Cobalt Singleâ€Atom Sites Derived from<br>Metal–Organic Frameworks: Enhanced Oxygen Reduction Performance. Angewandte Chemie, 2021, 133,<br>3249-3258.       | 2.0  | 44        |
| 131 | Rational design of Fe-N-C electrocatalysts for oxygen reduction reaction: From nanoparticles to single atoms. Nano Research, 2022, 15, 1753-1778.  | 10.4 | 44        |
| 132 | Metal single-atom catalysts for selective hydrogenation of unsaturated bonds. Journal of Materials<br>Chemistry A, 2021, 9, 5296-5319.   | 10.3 | 43        |
| 133 | Single-atom Sn-Zn pairs in CuO catalyst promote dimethyldichlorosilane synthesis. National Science<br>Review, 2020, 7, 600-608.  | 9.5  | 42        |
| 134 | Inâ€Situ Thermal Atomization To Convert Supported Nickel Nanoparticles into Surfaceâ€Bound Nickel<br>Singleâ€Atom Catalysts. Angewandte Chemie, 2018, 130, 14291-14296.  | 2.0  | 41        |
| 135 | Evolution of Hollow CuInS <sub>2</sub> Nanododecahedrons via Kirkendall Effect Driven by Cation<br>Exchange for Efficient Solar Water Splitting. ACS Applied Materials & Interfaces, 2019, 11,<br>27170-27177. | 8.0  | 40        |
| 136 | Electrochemical conversion of bulk platinum into platinum single-atom sites for the hydrogen evolution reaction. Journal of Materials Chemistry A, 2020, 8, 10755-10760.                                       | 10.3 | 40        |
| 137 | Structural revolution of atomically dispersed Mn sites dictates oxygen reduction performance. Nano Research, 2021, 14, 4512-4519.  | 10.4 | 40        |
| 138 | Au@HgxCd1-xTe core@shell nanorods by sequential aqueous cation exchange for near-infrared photodetectors. Nano Energy, 2019, 57, 57-65.  | 16.0 | 38        |
| 139 | Research progress of asymmetrically coordinated single-atom catalysts for electrocatalytic reactions. Journal of Materials Chemistry A, 2022, 10, 14732-14746.   | 10.3 | 38        |
| 140 | Self-assembly of ultrathin Cu <sub>2</sub> MoS <sub>4</sub> nanobelts for highly efficient visible light-driven degradation of methyl orange. Nanoscale, 2015, 7, 17998-18003.                                 | 5.6  | 36        |
| 141 | Dynamic evolution of isolated Ru–FeP atomic interface sites for promoting the electrochemical hydrogen evolution reaction. Journal of Materials Chemistry A, 2020, 8, 22607-22612.                             | 10.3 | 36        |
| 142 | A single-atom Cu–N <sub>2</sub> catalyst eliminates oxygen interference for electrochemical sensing of hydrogen peroxide in a living animal brain. Chemical Science, 2021, 12, 15045-15053.                    | 7.4  | 36        |
| 143 | A highly accessible copper single-atom catalyst for wound antibacterial application. Nano Research, 2021, 14, 4808-4813.   | 10.4 | 35        |
| 144 | 2D MOF induced accessible and exclusive Co single sites for an efficient <i>O</i> -silylation of alcohols with silanes. Chemical Communications, 2019, 55, 6563-6566.  | 4.1  | 34        |

| #   | Article  | IF   | CITATIONS |
|-----|--|------|-----------|
| 145 | Structure–Property Evolution of Poly(ethylene terephthalate) Fibers in Industrialized Process under<br>Complex Coupling of Stress and Temperature Field. Macromolecules, 2019, 52, 565-574.                                      | 4.8  | 34        |
| 146 | Selective Hydrogenation on a Highly Active Single-Atom Catalyst of Palladium Dispersed on Ceria<br>Nanorods by Defect Engineering. ACS Applied Materials & Interfaces, 2020, 12, 57569-57577.                                    | 8.0  | 34        |
| 147 | Notched-Polyoxometalate Strategy to Fabricate Atomically Dispersed Ru Catalysts for Biomass Conversion. ACS Catalysis, 2021, 11, 2669-2675.  | 11.2 | 34        |
| 148 | Oxidative desulfurization of dibenzothiophene with molecular oxygen catalyzed by carbon<br>fiber-supported iron phthalocyanine. Reaction Kinetics, Mechanisms and Catalysis, 2014, 111, 535-547.                                 | 1.7  | 32        |
| 149 | Visible-light responsive electrospun nanofibers based on polyacrylonitrile-dispersed graphitic carbon<br>nitride. RSC Advances, 2015, 5, 86505-86512.  | 3.6  | 32        |
| 150 | Efficient and Robust Hydrogen Evolution: Phosphorus Nitride Imide Nanotubes as Supports for<br>Anchoring Single Ruthenium Sites. Angewandte Chemie, 2018, 130, 9639-9644.  | 2.0  | 31        |
| 151 | Direct Synthesis of Atomically Dispersed Palladium Atoms Supported on Graphitic Carbon Nitride for<br>Efficient Selective Hydrogenation Reactions. ACS Applied Materials & Interfaces, 2020, 12,<br>54146-54154.                 | 8.0  | 31        |
| 152 | Highly Active and Stable Palladium Single-Atom Catalyst Achieved by a Thermal Atomization Strategy<br>on an SBA-15 Molecular Sieve for Semi-Hydrogenation Reactions. ACS Applied Materials &<br>Interfaces, 2021, 13, 2530-2537. | 8.0  | 31        |
| 153 | Interfacial peroxidase-like catalytic activity of surface-immobilized cobalt phthalocyanine on multiwall carbon nanotubes. RSC Advances, 2015, 5, 9374-9380.   | 3.6  | 30        |
| 154 | The coupling of hemin with persistent free radicals induces a nonradical mechanism for oxidation of pollutants. Chemical Communications, 2016, 52, 9566-9569.  | 4.1  | 30        |
| 155 | Revealing the Active Species for Aerobic Alcohol Oxidation by Using Uniform Supported Palladium<br>Catalysts. Angewandte Chemie, 2018, 130, 4732-4736.   | 2.0  | 29        |
| 156 | Semiconductor Nanocrystal Engineering by Applying Thiol―and Solventâ€Coordinated Cation Exchange<br>Kinetics. Angewandte Chemie - International Edition, 2019, 58, 4852-4857.  | 13.8 | 29        |
| 157 | Design of a Singleâ€Atom Indium δ+ –N 4 Interface for Efficient Electroreduction of CO 2 to Formate.<br>Angewandte Chemie, 2020, 132, 22651-22655.   | 2.0  | 29        |
| 158 | Theoretical Predictions, Experimental Modulation Strategies, and Applications of MXene‧upported<br>Atomically Dispersed Metal Sites. Small, 2022, 18, e2105883.  | 10.0 | 28        |
| 159 | Electrocatalytic acidic oxygen evolution reaction: From nanocrystals to single atoms. Aggregate, 2021, 2, e106.  | 9.9  | 27        |
| 160 | Colored TiO2 composites embedded on fabrics as photocatalysts: Decontamination of formaldehyde and deactivation of bacteria in water and air. Chemical Engineering Journal, 2019, 375, 121949.                                   | 12.7 | 26        |
| 161 | Raman scattering of single crystal Cu2MoS4 nanosheet. AIP Advances, 2015, 5, 037141.   | 1.3  | 25        |
| 162 | Atomically Dispersed Ruthenium Species Inside Metal–Organic Frameworks: Combining the High<br>Activity of Atomic Sites and the Molecular Sieving Effect of MOFs. Angewandte Chemie, 2019, 131,<br>4315-4319.                     | 2.0  | 25        |

| #   | Article   | IF   | CITATIONS |
|-----|---|------|-----------|
| 163 | Ordered Porous Nitrogenâ€Doped Carbon Matrix with Atomically Dispersed Cobalt Sites as an Efficient<br>Catalyst for Dehydrogenation and Transfer Hydrogenation of Nâ€Heterocycles. Angewandte Chemie,<br>2018, 130, 11432-11436.  | 2.0  | 24        |
| 164 | RuO2 clusters derived from bulk SrRuO3: Robust catalyst for oxygen evolution reaction in acid. Nano Research, 2022, 15, 1959-1965.  | 10.4 | 23        |
| 165 | Cube-like Cu2MoS4 photocatalysts for visible light-driven degradation of methyl orange. AIP<br>Advances, 2015, 5, 077130.   | 1.3  | 22        |
| 166 | Copper-based single-atom alloys for heterogeneous catalysis. Chemical Communications, 2021, 57, 2710-2723.  | 4.1  | 22        |
| 167 | Free Channel Formation around Graphitic Carbon Nitride Embedded in Porous Polyethylene<br>Terephthalate Nanofibers with Excellent Reusability for Eliminating Antibiotics under Solar<br>Irradiation. Industrial & Engineering Chemistry Research, 2017, 56, 11151-11160. | 3.7  | 21        |
| 168 | Compressive surface strained atomic-layer Cu2O on Cu@Ag nanoparticles. Nano Research, 2019, 12, 1187-1192.  | 10.4 | 21        |
| 169 | Facile synthesis of CoNi <sub>x</sub> nanoparticles embedded in nitrogen–carbon frameworks for<br>highly efficient electrocatalytic oxygen evolution. Chemical Communications, 2017, 53, 12177-12180.   | 4.1  | 20        |
| 170 | Porous platinum–silver bimetallic alloys: surface composition and strain tunability toward enhanced electrocatalysis. Nanoscale, 2018, 10, 21703-21711.   | 5.6  | 20        |
| 171 | From Indiumâ€Doped Ag <sub>2</sub> S to AgInS <sub>2</sub> Nanocrystals: Lowâ€Temperature In Situ<br>Conversion of Colloidal Ag <sub>2</sub> S Nanoparticles and Their NIR Fluorescence. Chemistry - A<br>European Journal, 2018, 24, 13676-13680.                        | 3.3  | 20        |
| 172 | Optimized MoP with Pseudo-Single-Atom Tungsten for Efficient Hydrogen Electrocatalysis. Chemistry of Materials, 2021, 33, 3639-3649.  | 6.7  | 20        |
| 173 | Silver based single atom catalyst with heteroatom coordination environment as high performance oxygen reduction reaction catalyst. Nano Research, 2022, 15, 7968-7975.  | 10.4 | 20        |
| 174 | Electrocatalytic degradation of organic contaminants using carbon fiber coupled with cobalt phthalocyanine electrode. Journal of Applied Electrochemistry, 2016, 46, 583-592.   | 2.9  | 19        |
| 175 | Phosphine ligand-mediated kinetics manipulation of aqueous cation exchange: a case study on the<br>synthesis of Au@SnS <sub>x</sub> core–shell nanocrystals for photoelectrochemical water<br>splitting. Chemical Communications, 2018, 54, 9993-9996.                    | 4.1  | 19        |
| 176 | Transforming cobalt hydroxide nanowires into single atom site catalysts. Nano Energy, 2021, 83, 105799.   | 16.0 | 19        |
| 177 | Insights into the generation of high-valent copper-oxo species in ligand-modulated catalytic system for oxidizing organic pollutants. Chemical Engineering Journal, 2016, 304, 1000-1008.   | 12.7 | 18        |
| 178 | Unique Cation Exchange in Nanocrystal Matrix via Surface Vacancy Engineering Overcoming Chemical<br>Kinetic Energy Barriers. CheM, 2020, 6, 3086-3099.  | 11.7 | 18        |
| 179 | High-Performance Quantum Dots with Synergistic Doping and Oxide Shell Protection Synthesized by<br>Cation Exchange Conversion of Ternary-Composition Nanoparticles. Journal of Physical Chemistry<br>Letters, 2019, 10, 2606-2615.  | 4.6  | 17        |
| 180 | Atomic-dispersed platinum anchored on porous alumina sheets as an efficient catalyst for diboration of alkynes. Chemical Communications, 2020, 56, 3127-3130.   | 4.1  | 17        |

| #   | Article  | IF   | CITATIONS |
|-----|--|------|-----------|
| 181 | Hollow anisotropic semiconductor nanoprisms with highly crystalline frameworks for<br>high-efficiency photoelectrochemical water splitting. Journal of Materials Chemistry A, 2019, 7,<br>8061-8072.                                   | 10.3 | 16        |
| 182 | Negative Pressure Pyrolysis Induced Highly Accessible Single Sites Dispersed on 3D Graphene<br>Frameworks for Enhanced Oxygen Reduction. Angewandte Chemie, 2020, 132, 20645-20649.  | 2.0  | 16        |
| 183 | Electron-rich isolated Pt active sites in ultrafine PtFe3 intermetallic catalyst for efficient alkene hydrosilylation. Journal of Catalysis, 2021, 396, 351-359.   | 6.2  | 16        |
| 184 | Single-Atom Ru on Al <sub>2</sub> O <sub>3</sub> for Highly Active and Selective 1,2-Dichloroethane<br>Catalytic Degradation. ACS Applied Materials & Interfaces, 2021, 13, 53683-53690.   | 8.0  | 16        |
| 185 | Construction of interconnected NiO/CoFe alloy nanosheets for overall water splitting. Renewable<br>Energy, 2022, 194, 459-468.   | 8.9  | 15        |
| 186 | Hydroxyl Radical-Dominated Catalytic Oxidation in Neutral Condition by Axially Coordinated Iron<br>Phthalocyanine on Mercapto-Functionalized Carbon Nanotubes. Industrial & Engineering<br>Chemistry Research, 2017, 56, 2899-2907.    | 3.7  | 14        |
| 187 | Atomically dispersed Ru in Pt <sub>3</sub> Sn intermetallic alloy as an efficient methanol oxidation electrocatalyst. Chemical Communications, 2021, 57, 2164-2167.  | 4.1  | 14        |
| 188 | Synergistic effects of silica nanoparticles and reactive compatibilizer on the compatibilization of polystyrene/polyamide 6 blends. Polymer Engineering and Science, 2017, 57, 1301-1310.  | 3.1  | 13        |
| 189 | Crystallization and Thermal Behaviors of Poly(ethylene terephthalate)/Bisphenols Complexes through<br>Melt Post-Polycondensation. Polymers, 2020, 12, 3053.  | 4.5  | 13        |
| 190 | Confined crystallization, melting behavior and morphology in PEGâ€ <i>b</i> â€PLA diblock copolymers:<br>Amorphous versus crystalline PLA. Journal of Polymer Science, 2020, 58, 455-465.  | 3.8  | 13        |
| 191 | Rational Control of the Selectivity of a Ruthenium Catalyst for Hydrogenation of 4â€Nitrostyrene by<br>Strain Regulation. Angewandte Chemie, 2017, 129, 12133-12137.   | 2.0  | 12        |
| 192 | PtAl truncated octahedron nanocrystals for improved formic acid electrooxidation. Chemical Communications, 2018, 54, 3951-3954.  | 4.1  | 12        |
| 193 | Effect of Protective Agents upon the Catalytic Property of Platinum Nanocrystals. ChemCatChem, 2018, 10, 2433-2441.  | 3.7  | 12        |
| 194 | Electrodeposition of polypyrrole on He plasma etched carbon nanotube films for electrodes of<br>flexible all-solid-state supercapacitor. Journal of Solid State Electrochemistry, 2019, 23, 1553-1562.                                 | 2.5  | 12        |
| 195 | Phase and interface engineering of nickel carbide nanobranches for efficient hydrogen oxidation catalysis. Journal of Materials Chemistry A, 2021, 9, 26323-26329.   | 10.3 | 12        |
| 196 | High-Valent Iron-Oxo Complexes as Dominant Species to Eliminate Pharmaceuticals and<br>Chloride-Containing Intermediates by the Activation of Peroxymonosulfate Under Visible Irradiation.<br>Catalysis Letters, 2020, 150, 1355-1367. | 2.6  | 11        |
| 197 | Controllable drilling by corrosive Cu1Ox to access highly accessible single-site catalysts for bacterial disinfection. Applied Catalysis B: Environmental, 2021, 293, 120228.  | 20.2 | 11        |
| 198 | Surface Molecular Encapsulation with Cyclodextrin in Promoting the Activity and Stability of Fe<br>Singleâ€Atom Catalyst for Oxygen Reduction Reaction. Energy and Environmental Materials, 2023, 6, .                                 | 12.8 | 11        |

| #   | Article   | IF   | CITATIONS |
|-----|---|------|-----------|
| 199 | Enhanced catalytic decoloration of Rhodamine B based on 4â€aminopyridine iron coupled with cellulose fibers. Journal of Chemical Technology and Biotechnology, 2015, 90, 1144-1151.   | 3.2  | 10        |
| 200 | Edge-Contact Geometry and Anion-Deficit Construction for Activating Ultrathin MoS <sub>2</sub> on<br>W <sub>17</sub> O <sub>47</sub> in the Hydrogen Evolution Reaction. Inorganic Chemistry, 2019, 58,<br>11241-11247.         | 4.0  | 10        |
| 201 | Micro-scale 2D quasi-nanosheets formed by 0D nanocrystals: from single to multicomponent building blocks. Science China Materials, 2020, 63, 1265-1271.   | 6.3  | 10        |
| 202 | Artificial light-harvesting 2D photosynthetic systems with iron phthalocyanine/graphitic carbon<br>nitride composites for highly efficient CO <sub>2</sub> reduction. Catalysis Science and Technology,<br>2021, 11, 5952-5961. | 4.1  | 10        |
| 203 | Atomically dispersed Pd catalysts promote the oxygen evolution reaction in acidic media. Chemical Communications, 2021, 57, 11561-11564.  | 4.1  | 10        |
| 204 | Flexible Electron-Rich Ion Channels Enable Ultrafast and Stable Aqueous Zinc-Ion Storage. ACS Applied<br>Materials & Interfaces, 2021, 13, 54096-54105.   | 8.0  | 10        |
| 205 | Atomic-Scale Tailoring and Molecular-Level Tracking of Oxygen-Containing Tungsten Single-Atom<br>Catalysts with Enhanced Singlet Oxygen Generation. ACS Applied Materials & Interfaces, 2021, 13,<br>37142-37151.               | 8.0  | 9         |
| 206 | Semiconductor Nanocrystal Engineering by Applying Thiol―and Solventâ€Coordinated Cation Exchange<br>Kinetics. Angewandte Chemie, 2019, 131, 4906-4911.  | 2.0  | 8         |
| 207 | A rational design of an efficient counter electrode with the<br>Co/Co <sub>1</sub> P <sub>1</sub> N <sub>3</sub> atomic interface for promoting catalytic<br>performance. Materials Chemistry Frontiers, 2021, 5, 3085-3092.    | 5.9  | 8         |
| 208 | Abiotic degradation behavior of polyacrylonitrile-based material filled with a composite of TiO2 and g-C3N4 under solar illumination. Chemosphere, 2022, 299, 134375.   | 8.2  | 8         |
| 209 | Constructing the separation pathway for photo-generated carriers by diatomic sites decorated on MIL-53-NH2(Al) for enhanced photocatalytic performance. Nano Research, 0, , .   | 10.4 | 8         |
| 210 | Enhanced removal of acid red 1 with large amounts of dyeing auxiliaries: the pivotal role of cellulose support. Cellulose, 2014, 21, 2073-2087.   | 4.9  | 6         |
| 211 | Innenrücktitelbild: Isolated Single Iron Atoms Anchored on Nâ€Doped Porous Carbon as an Efficient<br>Electrocatalyst for the Oxygen Reduction Reaction (Angew. Chem. 24/2017). Angewandte Chemie, 2017,<br>129, 7107-7107.      | 2.0  | 6         |
| 212 | Numerical simulation of the behavior of highâ€viscosity fluids falling film flow down the vertical wavy wall. Asia-Pacific Journal of Chemical Engineering, 2017, 12, 97-109.   | 1.5  | 6         |
| 213 | Revealing the role of graphene in enhancing the catalytic performance of phthalocyanine immobilized graphene/bacterial cellulose nanocomposite. Cellulose, 2019, 26, 7863-7875.   | 4.9  | 6         |
| 214 | Continuous postâ€polycondensation of highâ€viscosity poly(ethylene terephthalate) in the molten state.<br>Journal of Applied Polymer Science, 2019, 136, 47484.   | 2.6  | 6         |
| 215 | Fabrication of a wrinkled structure made of wearable polyacrylonitrile/polyurethane composite fibers with elastic sensing properties suitable for human movement detection. Polymer Composites, 2020, 41, 3491-3500.            | 4.6  | 6         |
| 216 | Film reaction kinetics for melt postpolycondensation of poly(ethylene terephthalate). Journal of<br>Applied Polymer Science, 2020, 137, 48988.  | 2.6  | 6         |

| #   | Article  | IF  | CITATIONS |
|-----|--|-----|-----------|
| 217 | Degradation of carbamazepine by MWCNTs-promoted generation of high-valent iron-oxo species in a<br>mild system with O-bridged iron perfluorophthalocyanine dimers. Journal of Environmental Sciences,<br>2021, 99, 260-266.                        | 6.1 | 6         |
| 218 | Solar-driven zinc-doped graphitic carbon nitride photocatalytic fibre for simultaneous removal of<br>hexavalent chromium and pharmaceuticals. Environmental Technology (United Kingdom), 2022, 43,<br>2569-2580.                                   | 2.2 | 6         |
| 219 | High-valent iron-oxo species on pyridine-containing MWCNTs generated in a solar-induced H2O2 activation system for the removal of antimicrobials. Chemosphere, 2021, 273, 129545.  | 8.2 | 6         |
| 220 | Structure and properties of gelâ€spun ultraâ€high molecular weight polyethylene fibers obtained from<br>industrial production line. Journal of Applied Polymer Science, 2021, 138, 51317.  | 2.6 | 6         |
| 221 | In Situ Implanting of Single Tungsten Sites into Defective UiOâ€66(Zr) by Solventâ€Free Route for Efficient<br>Oxidative Desulfurization at Room Temperature. Angewandte Chemie, 2021, 133, 20481-20487.   | 2.0 | 6         |
| 222 | Alkyne Semihydrogenation over Pd Nanoparticles Embedded in N,S-Doped Carbon Nanosheets. ACS<br>Applied Nano Materials, 2021, 4, 9052-9059.   | 5.0 | 6         |
| 223 | Carbon-Based Oxamate Cobalt(III) Complexes as Bioenzyme Mimics for Contaminant Elimination in High<br>Backgrounds of Complicated Constituents. Materials, 2017, 10, 1169.  | 2.9 | 5         |
| 224 | Nearâ€Infrared Luminescent Ternary Ag <sub>3</sub> SbS <sub>3</sub> Quantum Dots by in situ<br>Conversion of Ag Nanocrystals with Sb(C <sub>9</sub> H <sub>19</sub> COOS) <sub>3</sub> . Chemistry<br>- A European Journal, 2018, 24, 18643-18647. | 3.3 | 5         |
| 225 | Bottom-up pore-generation strategy modulated active nitrogen species for oxygen reduction reaction.<br>Materials Chemistry Frontiers, 2021, 5, 2684-2693.  | 5.9 | 4         |
| 226 | Reaction kinetics of melt postâ€polycondensation process for polycarbonate in film state. Journal of<br>Applied Polymer Science, 2022, 139, 51731.   | 2.6 | 4         |
| 227 | Construction of Synergistic Co and Cu Diatomic Sites for Enhanced Higher Alcohol Synthesis. CCS<br>Chemistry, 2023, 5, 851-864.  | 7.8 | 4         |
| 228 | Generation of reactive cobalt oxo oxamate radical species for biomimetic oxidation of contaminants.<br>RSC Advances, 2017, 7, 42875-42883.   | 3.6 | 3         |
| 229 | Interpenetratingâ€Syncretic Microâ€Nano Hierarchy Fibers for Effective Fine Particle Capture. Advanced<br>Engineering Materials, 2019, 21, 1801361.  | 3.5 | 3         |
| 230 | Two-dimensional CdX (X = Se, Te) nanosheets: controlled synthesis and their photoluminescence properties. Journal of Materials Chemistry C, 2019, 7, 13849-13858.  | 5.5 | 3         |
| 231 | Confined crystallization and melting behaviors of poly(ethylene glycol) endâ€functionalized by hydrogen bonding groups: Effect of contents for functional units. Polymer Crystallization, 2020, 3, e10158.   | 0.8 | 3         |
| 232 | Hydrodynamics and mixing performance in a continuous miniature conical counter-rotating twin-screw extruder. International Journal of Chemical Reactor Engineering, 2022, .  | 1.1 | 3         |
| 233 | Catalytic degradation of sulfaquinoxalinum by polyester/poly-4-vinylpyridine nanofibers-supported iron phthalocyanine. Environmental Science and Pollution Research, 2018, 25, 5902-5910.  | 5.3 | 2         |
| 234 | Biomimetic polydopamine catalyst with redox activity for oxygen-promoted H <sub>2</sub><br>production <i>via</i> aqueous formaldehyde reforming. Sustainable Energy and Fuels, 2021, 5,<br>4575-4579.  | 4.9 | 2         |

| #   | Article   | IF              | CITATIONS     |
|-----|---|-----------------|---------------|
| 235 | A general strategy to prepare atomically dispersed biomimetic catalysts based on host–guest<br>chemistry. Chemical Communications, 2021, 57, 1895-1898.   | 4.1             | 2             |
| 236 | Efficient peroxymonosulfate activation by N-rich pyridyl-iron phthalocyanine derivative for the elimination of pharmaceutical contaminants under solar irradiation. Chemosphere, 2022, 299, 134464.   | 8.2             | 2             |
| 237 | Saltâ€Induced Changes in Solâ€toâ€Gel Transition and Structure of Stereocomplexable Poly(lactic) Tj ETQq1 1 (   | ).784314<br>2.2 | rgBT /Overloc |
| 238 | Oxygen Reduction Reaction: MnN <sub>4</sub> Oxygen Reduction Electrocatalyst: Operando<br>Investigation of Active Sites and High Performance in Zinc–Air Battery (Adv. Energy Mater. 6/2021).<br>Advanced Energy Materials, 2021, 11, 2170025. | 19.5            | 0             |
| 239 | Frontispiece: In Situ Implanting of Single Tungsten Sites into Defective UiOâ€66(Zr) by Solventâ€Free Route<br>for Efficient Oxidative Desulfurization at Room Temperature. Angewandte Chemie - International<br>Edition, 2021, 60, .           | 13.8            | 0             |
| 240 | Frontispiz: In Situ Implanting of Single Tungsten Sites into Defective UiOâ€66(Zr) by Solventâ€Free Route<br>for Efficient Oxidative Desulfurization at Room Temperature. Angewandte Chemie, 2021, 133, .                                       | 2.0             | 0             |
| 241 | Effects of physical aging on the selfâ€healing, shape memory, and crystallization behaviors of<br>hydrogenâ€bonded supramolecular polymers. Journal of Polymer Science. 0. , .  | 3.8             | 0             |